ELSEVIER

NeuroToxicology 25 (2004) 1013–1030

NeuroToxicology

Physiologically Based Pharmacokinetic/ Pharmacodynamic Model for the Organophosphorus Pesticide Diazinon

T.S. Poet*, A.A. Kousba, S.L. Dennison, C. Timchalk

Center for Biological Monitoring and Modeling, Battelle, Pacific Northwest Division, PO Box 999 MSIN P7-59, Richland, WA 99352, USA

Received 8 October 2003; accepted 12 March 2004
Available online 23 April 2004

Abstract

Diazinon (DZN) is an organophosphorus pesticide with the possibility for widespread exposures. The toxicological effects of DZN are primarily mediated through the effects of its toxic metabolite, DZN-oxon on acetylcholinesterases, which results in accumulation of acetylcholine at neuronal junctions. A physiologically based pharmacokinetic/ pharmacodynamic (PBPK/PD) model was developed to quantitatively assess the kinetics of DZN and its metabolites in blood and the inhibition of cholinesterases in plasma, RBC, brain, and diaphragm. Focused in vivo pharmacokinetic studies were conducted in male Sprague–Dawley rats and the data were used to refine the model. No overt toxicity was noted following doses up to 100 mg/kg. However, cholinesterases in plasma, RBC, brain and diaphragm were substantially inhibited at doses of 50 mg/kg. In plasma, total cholinesterase was inhibited to less than 20% of control by 6 h post dosing with 100 mg/kg. Inhibition of brain acetylcholinesterase (AChE) following 100 mg/kg exposures was approximately 30% of control by 6 h. Diaphragm butyrylcholinesterase (BuChE) inhibition following 100 mg/kg dosing was to less than 20% of control by 6 h. The PBPK/PD model was used to describe the concentrations of DZN and its major, inactive metabolite, 2-isopropyl-4-methyl-6-hydroxypyrimidine (IMHP) in plasma and urinary elimination of IMHP. The fit of the model to plasma, RBC, brain, and diaphragm total cholinesterase and BuChE activity was also assessed and the model was further validated by fitting data from the open literature for intraperitoneal, intravenous, and oral exposures to DZN. The model was shown to quantitatively estimate target tissue dosimetry and cholinesterase inhibition following several routes of exposures. This model further confirms the usefulness of the model structure previously validated for chlorpyrifos and shows the potential utility of the model framework for other related organophosphate pesticides.

Keywords: Organophosphate pesticide; PBPK/PD; Cholinesterase inhibition

INTRODUCTION

Diazinon (DZN: *O,O*-diethyl-*O*-(2-isopropyl-4-methyl-6-pyrimidinyl) phosphorothionate]) is a commonly used thionophosphorus organophosphate (OP) pesticide. In addition to the anticipated exposures associated with pesticide use, DZN and other OPs have been found in many household and environmental samples, including; soil, house dust, and food residues (Butte and Heinzow, 2002; Lewis et al., 2001; MacIntosh et al., 2001).The ubiquitous nature of OP pesticides leads to a for significant OP exposure involving multiple routes. In this regard, DZN is an optimal candidate for PBPK/PD model development because of its extensive use, the existence of kinetic and metabolic studies in the literature, its mechanism of toxicity, and the ability to use blood/urinary metabolites and blood cholinesterase inhibition as quantitative biomarkers of exposure.

DZN is similar in chemical structure, mechanism of action, and metabolic profile to another OP for which a PBPK/PD model has already been developed (Timchalk

* Corresponding author. Tel.: +1-509-376-7740; fax: +1-509-376-9064.
E-mail address: torka.poet@pnl.gov (T.S. Poet).

0161-813X/$ – see front matter © 2004 Elsevier Inc. All rights reserved.
doi:10.1016/j.neuro.2004.03.002

et al., 2002b). The validity of the parameterization of the original chlorpyrifos model and the robustness of the current DZN model will be substantially improved by basing the underlying model structure on identical principles; a well-designed and functionally correct model for chlorpyrifos should also sufficiently describe DZN dosimetry and dynamics following chemical-specific parameterization. Since exposures to mixtures of OPs is likely, these individual models built on the same framework will impart the ability to develop binary models to describe dual exposures.

A review of the California pesticide use database for 1994 indicated that multiple OP pesticides are used to control pests in virtually all crop and commercial applications (i.e. nursery, lawn and garden) within the state (Cal EPA, 1998). Future aims will be to construct a mixture PBPK/PD model that describes the dosimetry and pharmacodynamics of concurrent exposures to chlorpyrifos and DZN. This mixture model can be readily modified, through focused research, to address the impact of variable OP exposure scenarios and the impact of sensitive sub-populations on the risk assessment for OP insecticides.

OP pesticides, like DZN, inhibit acetylcholinesterase (AChE) activity in nerve tissue, resulting in the accumulation of the neurotransmitter acetylcholine, producing excessive cholinergic stimulation and associated neurotoxicity, including increased urination/defecation, lethargy, and death (Lotti, 2001). While DZN itself has mild AChE inhibitory potential, its oxygenated metabolite, DZN-oxon is much more potent (Wilson, 2001). Differences in the ratio of activation to an oxygen analogue and metabolic detoxification are associated with sensitivity to OPs (Ma and Chambers, 1994; Timchalk et al., 2002a). A metabolic scheme for the metabolism of DZN is presented in Fig. 1. As illustrated, CYP450 enzymes catalyze both the activation of DZN to DZN-oxon as well as the detoxification of DZN to 2-isopropyl-4-methyl-6-hydroxypyrimidine (IMHP), and diethylthiophosphate. DZN-oxon is additionally detoxified by hepatic and extrahepatic A- and B-esterases to form IMHP and diethylphosphate (Fabrizi et al., 1999; Poet et al., 2003; Yang et al., 1971). A unique feature of PBPK/PD models is their capability to link dosimetry with biological response. This is important since a decrement in cholinesterase activity is routinely utilized as a biomonitor for human exposure to OPs as well as in toxicology studies in animals. The use of cholinesterase inhibition in risk assessments can result in a high level of conservatism since this parameter is sensitive to OP exposures, beyond a level at which toxicity is observed. The use of cholinesterase activity as a biomarker, linked to a PBPK model can eventually lead to a more accurate assessment of risk.

There are three classes of esterases, A, B, and C. A-esterases (PON; e.g. PON1) are not inactivated by the

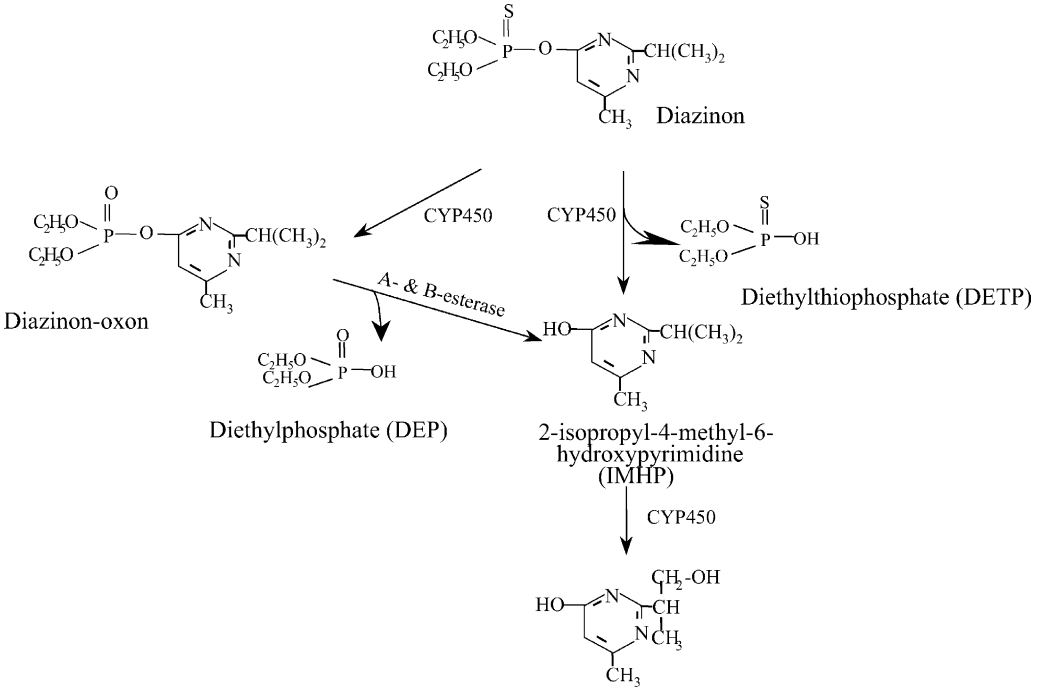

Fig. 1. Metabolic scheme for diazinon (DZN) and its major metabolites DZN-oxon and IMHP, and diethyl- and diethylthiophosphate.

OPs, but do detoxify the oxon metabolite. B-est[1] such as carboxylesterase, butyrylcholinesterase (BuChE), and AChE stochiometrically bind to the oxon and become inactivated (for a review see Wilson, 2001). C-esterases do not interact with OPs (Aldridge, 1971).Since esterases are distributed throughout the various tissues of the body, they contribute to the overall detoxification of DZN-oxon. Plasma and RBC cholinesterase activities are often used as dose-metrics for assessing OP exposures. Due to extensive metabolism, little, if any, DZN or DZN-oxon are available for excretion; however, more stable metabolites such as diethylthiophophate, diethylphosphate, and IMHP form the major metabolites and are readily excreted in the urine (Iverson et al., 1975; Mucke et al., 1970) and are thus potentially important biomarkers of exposure and dose.

It has previously been demonstrated that PBPK/PD models used to determine the relationships between OP dosimetry and B-est inhibition will be useful for assessing risk associated with OP exposure (Gearhart et al., 1990; Timchalk et al., 2002a). Quantification of urinary metabolites, such as IMHP, and blood cholinesterase inhibition can both be used as biomarkers for exposure, since the levels of IMHP and inhibition of cholinesterase are dependent upon the route and length of exposure, and metabolism and excretion of DZN and metabolites. Hence, it is clear that a PBPK/PD model for DZN can be used to link biomarkers of both dosimetry and dynamic response to quantitatively assess exposure.

This paper describes the development and validation of a PBPK/PD model for DZN and its metabolites based on a previous model for a related OP pesticide, chlorpyrifos (Timchalk et al., 2002a,b). These models have been designed to quantitatively integrate tissue dosimetry and dynamic response (cholinesterase inhibition) in blood and selected tissues with the pharmacokinetics of the OPs and their more stable metabolites. To develop the model, pharmacokinetic/pharmacodynamic studies were conducted in rats to assess dosimetry and dynamic response over a range of DZN doses. The model was also evaluated against available rodent and human dosimetry and cholinesterase inhibition data from the published literature.

MATERIALS AND METHODS

Chemicals

Chlorpyrifos was kindly provided by Dow AgroSciences (Indianapolis, IN, USA). Diazinon (98.5% pure), DZN-oxon (90% pure), and IMHP (99% pure) were purchased from Chem Service, Inc (West Chester, PA, USA). Toluene (99.8% pure) was purchased from Burdick and Jackson (Muskegon, MI, USA). Diazinon-oxon was stored at −80 °C until use, while all other test materials were stored at room temperature. The remaining chemicals used in this study were reagent grade or better and were purchased from Sigma (St. Louis, MO, USA).

Animals

Adult male Sprague–Dawley rats (275–325 g) were obtained from Charles River Inc. (Raleigh, NC, USA). Prior to use, animals were housed in solid-bottom cages with hardwood chips, and were acclimated in a humidity- and temperature-controlled room with a 12-h light/dark cycle. Deionized water (reverse osmosis) and PMI 5002 Certified Rodent Diet (Animal Specialties, Inc. Hubbard, OR) were provided *ad libitum*.

Animal Exposures

The time-course of DZN and IMHP in plasma and elimination of IMHP in urine were determined in Sprague–Dawley rats following oral administration of a dose solution prepared in corn oil at doses ranging from 15 to 500 mg DZN/kg body weight. All animals were fasted ∼16 h prior to administration of DZN and dosed between 8.00 and 9.30 a.m. Animals (5/time-point) were killed by CO_2 asphyxiation and tissues collected at 1, 3, 6, 12, and 24 h post-dosing. Blood was collected from the posterior vena cava into heparinized syringes and centrifuged to separate plasma and RBCs. Aliquots of whole blood were analyzed by gas chromatography (GC) for DZN and IMHP concentrations and cholinesterase activity was determined spectrophotometrically in plasma and RBCs. The diaphragm was removed from animals in the 50 and 100 mg/kg dose groups and quickly frozen in liquid nitrogen for cholinesterase activity determinations. An additional group of animals were treated with 500 mg/kg, sacrificed 6 h later and the brain AChE inhibition was estimated. All tissues were stored at −80 °C until analysis.

Chemical Analysis

An analytical method was developed to directly quantify DZN and IMHP in plasma and urine. Chlorpyrifos was used as an internal standard and plasma

[1] Both AChE and BuChE are cholinesterases (ChE).

and urine were extracted with toluene at a 1:1 ratio (v/v) at room temperature. The solutions were mixed well on a vortex mixer and layers were separated by centrifugation. A 1-ml aliquot of the extract was blown down under gentle N_2 stream and reconstituted in toluene (100 μl to 1 ml) to place the GC response within the linear range of the calibration curve. Samples were injected onto a Hewlett-Packard 5890 GC in duplicate, using an autosampler. The GC was equipped with nitrogen phosphorus (NPD) and flame ionization (FID) detectors. The NPD detector was used due to its increased sensitivity for DZN. Duplicate aliquots of 1 μl were injected onto the columns using an autosampler. Separation was achieved using a Stabilwax-DB column (15 m × 0.53 mm i.d. × 0.25 μm film thickness: Restek, Bellefonte, PA, USA). Hydrogen was used as the carrier gas with a head pressure of 5 psi. Helium was the makeup gas for the NPD detector while N_2 was the makeup gas for FID detector. The temperature was ramped at a rate of 15 °C/min from 65 to 165 °C, which was held for 2 min and then followed by a second ramp of 50 °C/min to the final temperature of 230 °C. The injector and detector temperatures were 275 and 300 °C, respectively. The retention times for DZN and IMHP were approximately 6.0 and 6.6 min, respectively. Detection limits were approximately 0.2 and 2 μM for DZN and IMHP, respectively.

Cholinesterase Analysis

Total cholinesterase and BuChE activity in diluted tissue homogenates were determined using the Ellman assay (Ellman et al., 1961) as it was modified for a 96-well plate reader (Mortensen et al., 1996) and described previously (Kousba et al., 2003). Briefly, samples were diluted to be within the linear range. For brain, plasma, diaphragm and RBC, the dilutions were approximately 1200, 90, 225 and 290 times, respectively. Wells contained 0.25 ml diluted tissue homogenate with dithiobisnitrobenzoate and either acetylthiocholine or butyrylthiocholine at final concentrations of 0.1 and 0.4 mM, respectively, and a final total volume of 300 μl. To determine specific BuChE activity, butyrylthiocholine was used as a substrate. Butyrylthiocholine is a specific substrate for BuChE (Kousba et al., 2003; Lassiter et al., 1998), although it may have very limited activity compared to acetylthiocholine (less than 1%) as a substrate for AChE (Taylor et al., 1995). Total cholinesterase activity was determined using acetylthiocholine as a substrate. The absorbance at 412 nm was monitored over 30–40 min and the linear portion of the profile of increasing absorbance with time was fitted with the equation for a straight line, and the slope of this line was used as a measurement of uninhibited cholinesterase and BuChE activity. Determination of RBC cholinesterase activity was estimated using 6,6′-dithionicotinic acid as a coupling agent rather than the Ellman agent (5,5′-dithiobis-nitrobenzoic acid) in order to avoid the hemoglobin interference at 412 nm wavelength (Hackathorn et al., 1983).

Model Structure

The model structure was based on absorption, distribution, metabolism, and excretion (ADME) data from the open literature and from previously published PBPK/PD models for related OPs (Gearhart et al., 1990; Timchalk et al., 2002b). A diagram of the PBPK/PD model structure is shown in Fig. 2. This model was developed to describe the ADME time-course of DZN, DZN-oxon and IMHP and the inhibition of target cholinesterases in rats and humans. The model assumes the pharmacokinetic response in rats and humans is independent of gender. For the purpose of this model, the competing CYP450 metabolism to DZN-oxon and IMHP was assumed to occur in the liver. Detoxification of DZN-oxon by PON was included in the blood and liver compartments, while B-est activity (AChE, BuChE and carboxylesterase) was described in the blood, diaphragm, liver and brain compartments. Dermal and oral (gavage and dietary) routes of exposure were included to estimate dosimetry from potential environmental exposures; in addition, intravenous (i.v.) and intraperitoneal (i.p.) dosing was included to facilitate modeling of previously published studies in the rat. To develop and refine this model, focused pharmacokinetic and pharmacodynamic studies were conducted in rats (described in section ‘‘Animal Exposures’’), and the model was further evaluated against available dosimetry and dynamic response data from the open literature.

Physiological and metabolic parameters (i.e. tissue volume, blood flow and metabolic capacity) were scaled as a function of body weight according to the methods of Ramsey and Andersen (1984). Equations to describe the dermal uptake of DZN into the skin compartment of humans were adapted from Poet et al. (2000).

To develop any model, several parameter estimates are required, including: physiological constants, partition coefficients, and biochemical constants describing metabolism. These data were obtained from the literature, determined experimentally, or by optimization of model output utilizing the computer simulation. The

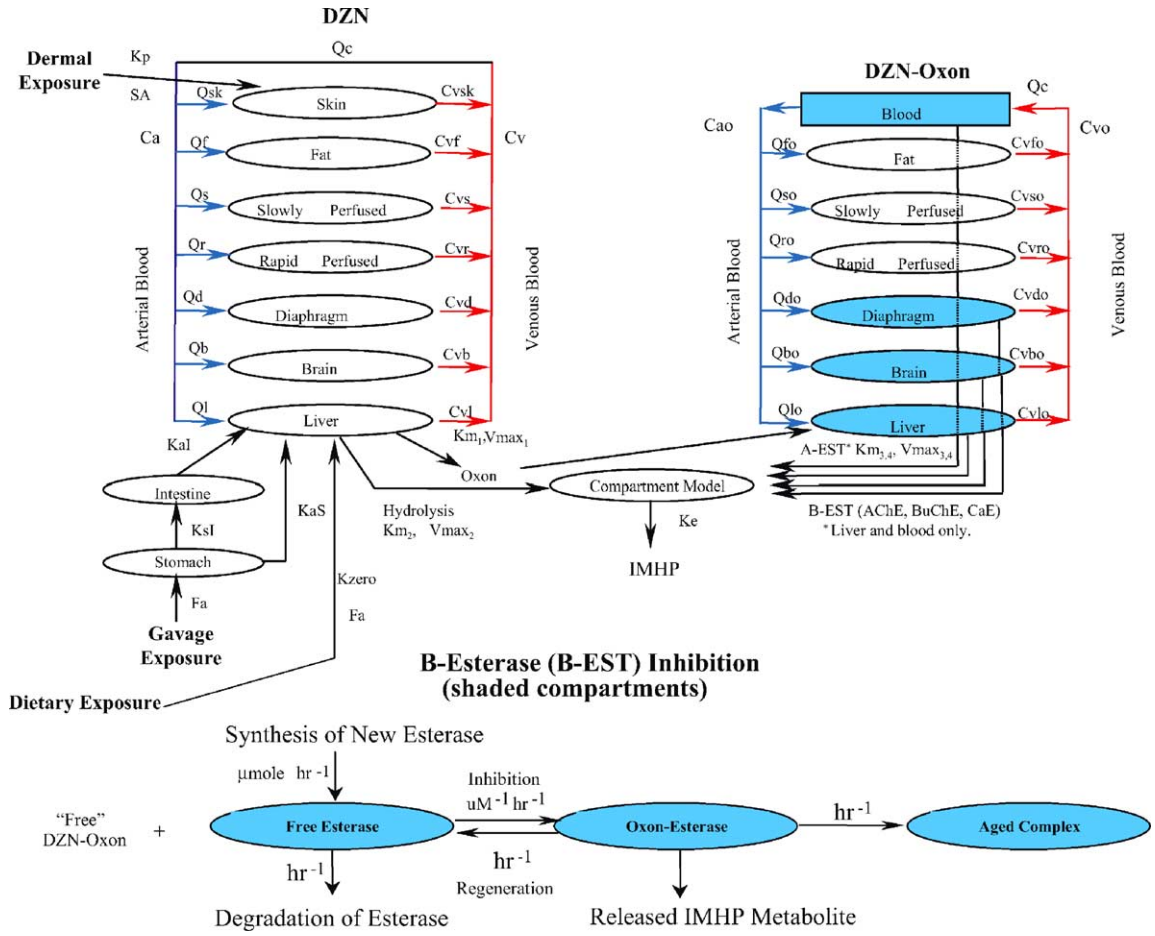

Fig. 2. PBPK/PD model, based on the model developed by Timchalk et al. (2002a,b), used to describe the disposition of DZN, DZN-oxon, and IMHP and the cholinesterase inhibition in rats and humans following oral and dermal exposures. The shaded compartments indicate tissues in which B-est (AChE, BuChe and carboxylesterase) enzyme activity is described. Model parameter definitions: Q_C: cardiac output (l/h); Q_i, blood flow to 'i' tissue (l/h); C_a, arterial blood concentration of DZN (µmole/L)' C_{vo}, pooled venous blood concentration of DZN-oxon (µmole/L); C_{vi}, venous blood concentration of DZN draining 'i' tissue (µmole/L)' C_{vio}, venous blood concentration of DZN-oxon draining 'i' tissue (µmole/L); SA, surface area of skin exposed (Cm2); K_P, skin permeability coefficient (cm/h); K_{zero}, zero-order rate of absorption of DZN from diet (µmole/h); F_a, fractional absorption (%) of gavage dose; K_{aS} and K_{aI}, first-order rate constant for absorption of DZN from compartments 1 and 2 (h^{-1}); K_{si}, first-order rate constant for transfer of DZN from compartments 1 and 2 (h^{-1}); K_e, first-order rate constant for elimination of IMHP from compartment 3; $K_{m(1–4)}$, Michaelis–Menten constant for saturable process (µmole/L); $V_{max(1–4)}$, maximum velocity for saturable process (µmole/(kg h)).

PBPK/PD model code for simultaneous solution of both algebraic and differential equations was developed in SIMUSOLV®, a computer program containing a numerical integration, optimization, and graphical routine, which is based on ACSL, a FORTRAN-based software. Organ volumes, cardiac output, and tissue blood flows were obtained from the literature (Brown et al., 1997) and are summarized in Table 1. The partition coefficients for DZN were determined using an algorithm developed by Poulin and Krishnan (1996). The values and references used for these parameters are listed in Table 2. This algorithm was also shown to be effective to determine partition coefficients for chlorpyrifos (Timchalk et al., 2002b).

Biochemical Constants

The CYP450 mediated metabolism of DZN to either oxon or IMHP was limited to the liver compartment and PON mediated metabolism was described in both the blood and liver, both PON and CYP450 metabolism were based on Michaelis–Menten kinetics. Parameter estimates for both CYP450 and PON metabolism of DZN and DZN-oxon were determined in vitro using hepatic microsomes in a previous study (Poet et al., 2003). The in vitro V_{max} for microsomal metabolism to oxon and IMHP were 0.38 and 2.8 nmole/(min mg) microsomal protein, respectively. The V_{max} for DZN metabolism by rat liver microsomes was extrapolated

Table 1
General physiological parameters used in the PBPK/PD model for DZN

	Rat	Human
Body wt (kg)	0.295–0.340	83
Tissue volume (% body weight)		
Blood[a]	6	7
Brain	1.2	2
Diaphragm	0.03	0.03
Liver	4.0	3.0
Rapidly perfused	4.0	4.0
Slowly perfused	78	63
Fat	7.0	21
Skin[b]	10.0	3.5
Flows (l/h)		
Alveolar ventilation	6.1–6.8	394
Cardiac output	6.1–6.8	394
Percentage of cardiac output		
Liver	25	23
Brain	3	11
Diaphragm	0.6	0.6
Rapidly perfused	43	40
Slowly perfused	14	14
Fat	9.0	5.0
Skin[b]	5.8	5.8

Parameters relating to the skin compartment were obtained from Jepson and McDougal (1997) and Brown et al. (1997).

[a] All parameters except those relating to the skin compartment were obtained from Brown et al. (1997).

[b] Values are for total skin. The skin compartment in the PBPK/PD model was comprised solely of the area of the skin under the exposure cell. The remainder of the skin was included in the slowly perfused compartment.

to the whole animal using values measured during microsomal preparation ($n = 6$ male rats) of an average of 15 g liver per rat, 394 g body weight (BW), and 25 mg microsomal protein/g liver. In addition, the V_{max} values used in PBPK models ($V_{max,C}$) are typically scaled to $BW^{0.74}$, which is a standard conversion used to describe the relationship between body surface area, body weight, and metabolic scaling in vivo.

The blood and urinary elimination of IMHP was described with a simple one-compartment model using a first-order rate constant to describe urinary excretion of IMHP. The one-compartment model was employed due to its reasonable fit to the data, the lack of tissue dosimetry data, the low number of parameters needed and the need of tracking only blood and urinary data for biomonitoring purposes. The selection of a reasonable set of elimination rate constants was determined by evaluating the overall goodness of fit of the model against the available experimental data in an iterative process. Once a reasonable set of elimination rate constants was determined, it was held constant throughout all data sets. The values and references used for these parameters are likewise listed in Table 2.

The model structure for the inhibition of cholinesterase by DZN-oxon in plasma, RBC, brain, and diaphragm was based on the model structure developed by Gearhart et al. (1990) for diisopropylfluorophosphate as it was modified by Timchalk et al. (2002b) for chlorpyrifos (see Fig. 2). Since chlorpyrifos and DZN are both phosphorothionates, model parameters for chlorpyrifos reactivation (K_r), and aging (K_a) originally from Carr and Chambers (1991) and validated in the PBPK/PD model for chlorpyrifos (Timchalk et al., 2002b) were incorporated into the DZN model. Since the leaving group from these similar pesticides is identical, the reactivation rates should be very close or identical and aging is solely dependent on enzyme kinetics, regardless of compound. Apparent bimolecular inhibition (K_i) parameters for AChE and BuChE blood and tissue activities were estimated by fitting the experimental data (Table 3). The initial estimates for diazinon-oxon interaction with B-esterases (AChE, BuChE and carboxylesterase) were based on the values determined by Timchalk et al., 2002a,b, describing CPF-oxon dynamics; however the final values were determined using model optimization against the available in vivo data or by using in vitro parameter estimation, when available.

The total amount of RBC AChE in the rat was calculated based on the experimentally determined total RBC AChE enzyme activity in control animals (Timchalk et al., 2002b). The recovery of RBC AChE enzyme activity was based on the rate of RBC replenishment, assuming a lifespan of 50 and 122 days in the rat and human, respectively, as described (Timchalk et al., 2002b).

RESULTS

Rat Pharmacokinetics/Pharmacodynamics

For target oral doses of 50 and 100 mg DZN/kg, actual doses administered were ~97% of target at 48.8 and 97.4 mg/kg, respectively. No overt toxicity was observed in any animal post-dosing. Oral absorption parameters that resulted in the best fit of the data are given in Table 2. Based upon in vitro ultrafiltration experiments, DZN was reported to be 89% bound to plasma proteins (Wu et al., 1996). This value was applied to the model by binding up DZN in the blood

Table 2
DZN-specific parameters used in the PBPK/PD model

Parameter	DZN	DZN-oxon	Estimation method[a]
Partition coefficients[b]			
Brain/blood	28	10	Calculated
Diaphragm/blood	5	2	Calculated
Fat/blood	360	120	Calculated
Liver/blood	18	7	Calculated
Rapid perfused/blood	8	2	Calculated
Slowly perfused/blood	5	2	Calculated
Skin/Blood	5	5	Calculated
Metabolic constants[c]			
CYP450 DZN-to-oxon (liver)			
$K_{m,1}$ (μmole/L)	25		Fitted
$V_{max,C1}$ (μmole/(h kg))	14		Measured
CYP450 DZN-to-IMHP			Measured
$K_{m,2}$ (μmole/L)	200		Measured
$V_{max,C2}$ (μmole/(h kg))	180		Measured
PON oxon-to-IMHP (liver)			Measured
$K_{m,3}$ (μmole/L)	270		Measured
$V_{max,C3}$ (μmole/(h kg))	63000		Measured
PON oxon-to-IMHP (blood)			Measured
$K_{m,4}$ (μmole/L)	270		Measured
$V_{max,C4}$ (μmole/(h kg))	63000		Measured
Oral absorption parameters (Wu et al., 1985[d])			
K_{aS} (stomach; h^{-1})	0.068	0.10	Fitted
K_{aI} (intestine; h^{-1})	0.058	0.59	Fitted
K_{si} (transfer stomach-intestine; h^{-1})	0.21	0.48	Fitted
F_a (fractional Abs.; %)	0.80	0.80	Fitted
Dermal absorption parameters (human)			
K_p (permeability coefficient; cm h^{-1})		1.3×10^{-4}	Fitted
IMHP model parameters (human)			
V_d (L)	0.25		Fitted
K_e (h^{-1})	0.29	12	Fitted
K_1 (first-order rate of loss)	0.55	0	
Plasma protein binding			
DZN (%)	0.89		Fixed[e]
DZN-oxon (%)	0.89		Fixed

[a] The model parameters were calculated using an algorithm (calculated), measured in independent experiments (measured), estimated by optimizing the model to the data (fitted), or fixed from reports in the literature (fixed).
[b] Partition coefficients were calculated based on the algorithm of Poulin and Krishnan (1996).
[c] Metabolic rate constants for the CYP450-mediated metabolism of DZN to IMHP or DZN-oxon and for the PON-mediated metabolism of DZN-oxon were determined in vitro (Poet et al., 2003) and scaled for use in the model as described in the text.
[d] Oral absorption parameters were optimized independently for data obtained in this study using an oil vehicle and data from the study of Wu et al., which employed a 5% Tween 20 vehicle.
[e] Wu et al. (1985).

compartment as a constant fraction. This simple binding format resulted in a reasonable fit to the data and no kinetic rate constants were used to describe dynamic binding. Although the extent of DZN-oxon plasma protein binding has not been determined experimentally, it was assumed that DZN-oxon would exhibit a similar fractional binding (see Table 2). The time-course of DZN in plasma and the model predictions are shown in Fig. 3. Measured peak blood levels at 3 h post-dosing were 559 ± 22.1 and 982 ± 190 nmole/L for the 50 and 100 mg/kg doses, respectively. The PBPK/PD model accurately predicted the overall DZN blood time-course profile and the simulated peak blood levels were 504 and 967 nmole/L, respectively.

The time-course of plasma IMHP concentrations was also quantified at 1, 3, 6, 12 and 24 h post-dosing

Table 3
Cholinesterase parameters used in the model

Enzyme turnover rate (Enz. Hydro./h)	
AChE	1.17E+07
BuChE	3.66E+06
Carboxylesterase	1.09E+05
Enzyme activity (μmole/(kg h))	
Brain AChE	4.40E+05
Diaphragm AChE	7.74E+04
Liver AChE	1.02E+04
Plasma AChE	1.32E+04
Brain BuChE	4.68E+04
Diaphragm BuChE	2.64E+04
Liver BuChE	3.00E+04
Plasma BuChE	1.56E+04
Brain carboxylesterase	6.00E+03
Diaphragm carboxylesterase	3.18E+05
Liver carboxylesterase	1.94E+06
Plasma carboxylesterase	4.56E+05
Enzyme degradation rate (h^{-1})	
$K_{d,1}$, brain AChE	0.01
$K_{d,2}$, diaphragm AChE	0.01
$K_{d,3}$, liver AChE	0.1
$K_{d,4}$, plasma AChE	0.1
$K_{d,5}$, RBC AChE	0.008
$K_{d,6}$, brain BuChE	0.01
$K_{d,7}$, diaphragm BuChE	0.01
$K_{d,8}$, liver BuChE	0.1
$K_{d,9}$, plasma BuChE	0.1
$K_{d,10}$, brain carboxylesterase	7.54E−04
$K_{d,11}$, diaphragm carboxylesterase	0.001
$K_{d,12}$, liver carboxylesterase	0.001
$K_{d,13}$, plasma carboxylesterase	0.0033
Bimolecular inhibition rate (μmole/h)[a]	
$K_{i,1–4}$, all tissues AChE	525
$K_{i,6–9}$, all tissues BuChE	1700
$K_{i,10}$, all tissues carboxylesterase	0.5
Reactivation rate (h^{-1})	
$K_{r,1–4}$, AChE	1.43E−02
$K_{r,5}$, RBC AChE	4.00E−02
$K_{r,6–9}$, BuChE	1.43E−02
$K_{r,10–13}$, carboxylesterase	1.43E−02
Aging rate (h^{-1})	
$K_{a,1–5}$, AChE	1.13E−02
$K_{a,6–9}$, BuChE	1.13E−02
$K_{a,10–13}$, carboxylesterase	1.13E−02
RBC life-span (days)	50

Except where noted ([a]), all parameters were obtained from the model for chlorpyrifos, as described previously (Timchalk et al., 2002b) and resulted in reasonable fits to the DZN data. basic.

[a] Inhibition rate constants (K_i) for DZN-oxon were optimized for this DZN model.

and urinary concentrations were quantified at 12 and 24 h (Fig. 4). These data indicate that DZN is extensively metabolized to IMHP. Peak plasma IMHP levels were reached at 3–6 h and the plasma IMHP

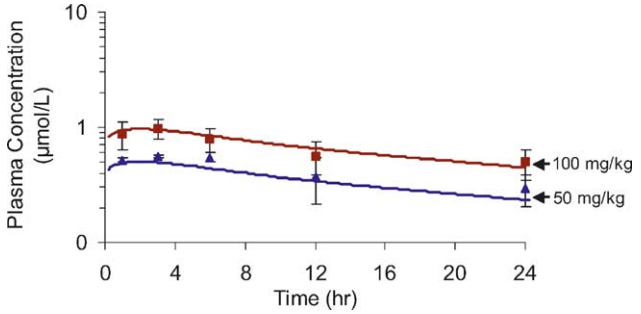

Fig. 3. Experimental data (symbols) and simulations (lines) for the concentration of DZN in the blood of rats administered DZN by oral gavage at dose levels of 50 (▲), 100 (■) mg/kg. The data represent the mean ± S.D. of five animals per treatment group.

concentrations were proportional to dose. The PBPK/PD model predicted that peak blood concentrations of 9.81 and 18.5 μmole/L IMHP would be achieved by 5 h post-dosing for the 50 and 100 mg/kg dose groups, respectively. Blood levels of IMHP were appreciably higher than levels of the DZN parent. Blood levels of DZN and IMHP were not quantified from the 15 mg/kg exposure due to analytical detection limits.

To fit the urinary and plasma IMHP data, a first-order process of elimination of IMHP in the 1-compartment submodel (See Fig. 2) due to further metabolism was also included. The model slightly under-predicted the

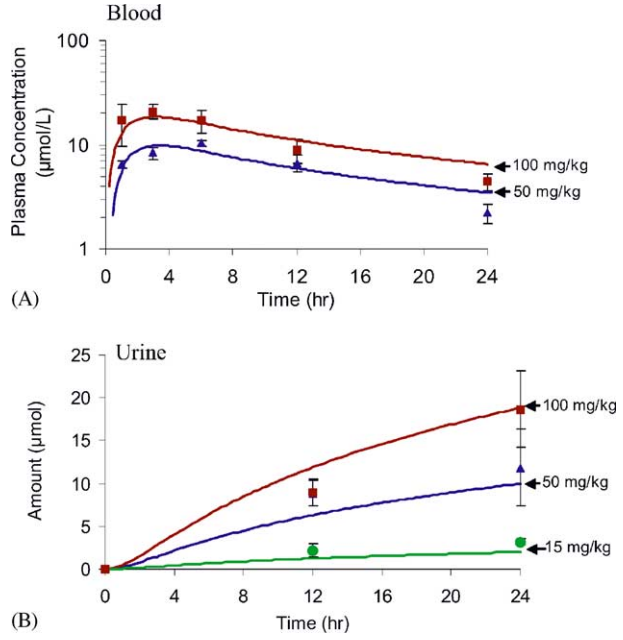

Fig. 4. Experimental data (symbols) and simulations (lines) for the blood kinetics and urinary elimination of IMHP in rats administered the DZN by oral gavage at dose levels of 15 (●), 50 (▲) and 100 (■) mg/kg. The data represent the mean ± S.D. of five animals per treatment group. Blood levels of IMHP were not measured from the 15 mg/kg dose due to analytical limits of detection.

amount of IMHP excreted for the 15 and 50 mg/kg dose groups. This may suggest that urinary elimination may follow a saturable process, rather than a first-order elimination. Since the data is limited to just 2 time points, the model was not modified to improve the fit and the more simple description of urinary elimination was maintained. The amount of IMHP formed was proportional to dose.

The ability of the model to predict the inhibition of AChE, BuChE and carboxylesterase in plasma, RBC, brain, and diaphragm were also assessed. To differentiate the contribution of AChE and BuChE from the total plasma cholinesterase response, acetylthiocholine was used as a substrate for total cholinesterase and butyrylthiocholine was used to specifically quantify BuChE inhibition. Inhibition rate constants for AChE, BuChE, and carboxylesterases were optimized in an iterative manner to best fit all data sets using the same parameter for each type of cholinesterase, regardless of tissue (Table 3). This methodology was used as an internal validation of the inhibition parameters, which should be more influenced by the type of esterase, and not be dependent upon tissue type. All other esterase parameters were held constant from the chlorpyrifos PBPK/PD model developed by Timchalk et al. (2002b). Due to the similarity of inhibition between the 15 and 50 mg/kg doses, it was necessary to use a lower Michaelis–Menten constant (K_M) to describe the production of oxon from the value determined in in vitro experiments (Table 2: Poet et al., 2003).

The time-course for plasma total cholinesterase, plasma BuChE, and RBC AChE inhibition following oral administration of 15, 50, and 100 mg DZN/kg of body weight are presented in Fig. 5. Plasma BuChE was not measured in the 15 mg/kg dose group. Model prediction of total cholinesterase activity in plasma (see Fig. 5A) were ~40–80% inhibited by 6 h post-dosing following oral exposure to 15, 50, and 100 mg DZN/kg, and showed minimal recovery through 24 h. The data from the 50 and 100 mg/kg dose groups appeared to be inverted. This could be due to sample collection error or to the similar extent of inhibition above 50 mg/kg and natural variability. The measured cholinesterase inhibition was greater than predicted by the model for the 15 mg/kg dose group. Plasma BuChE response was particularly sensitive to DZN (see Fig. 5B) since both the 50 and 100 mg/kg response showed near complete inhibition, which was maintained through 24 h post-dosing. The data indicated that the maximal level of RBC AChE inhibition was from ~20 to 60% following the 15, 50, and 100 mg DZN/kg doses, respectively, which represents less inhibition relative to the plasma

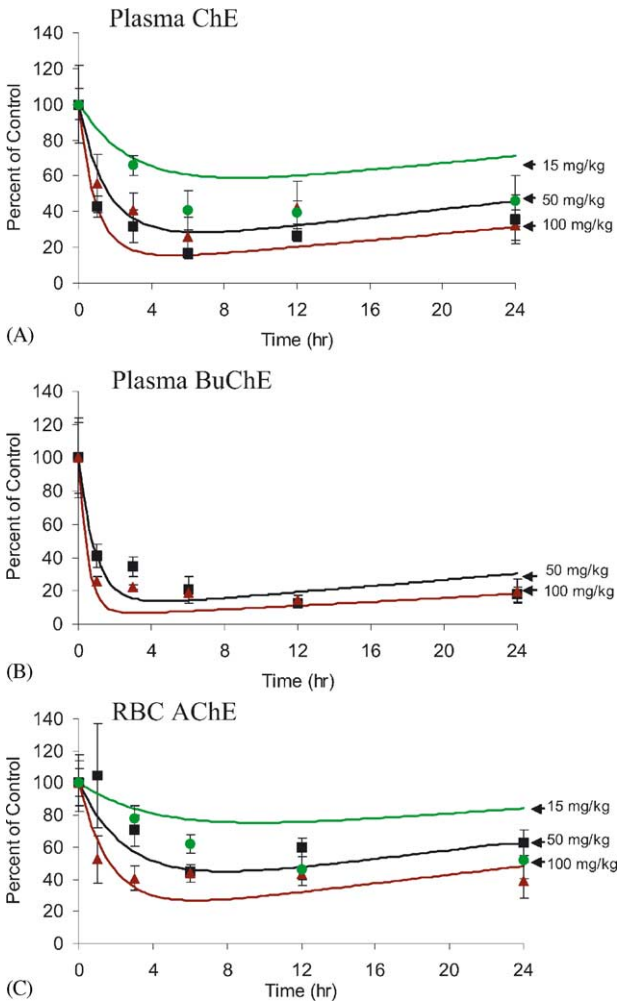

Fig. 5. Experimental data (symbols) and simulations (lines) for the inhibition of plasma total cholinesterase, BuChE, and RBC AChE in Sprague–Dawley rats administered DZN by oral gavage at doses of 15 (●), 50 (▲) and 100 (■) mg/kg. The data represent the mean ± S.D. of five animals per treatment group.

cholinesterase response. Similar to the plasma esterase inhibition compared to model predictions, measured inhibition was greater in RBCs than predicted by the model for the 15 mg/kg dose group.

Model parameterizations for the plasma cholinesterase and RBC AChE were based on a previous model by Maxwell et al. (1987) as it was modified by Timchalk et al. (2002b) and rate constants optimized to describe DZN-specific inhibition kinetics. For DZN-oxon the apparent bimolecular inhibition (K_i) rate constants for BuChE and AChE were determined to be 1700 and 525 $\mu M^{-1} h^{-1}$ by optimization of the cholinesterase and BuChE inhibition data sets, respectively. The K_i for carboxylesterase was set at 0.5 $\mu M^{-1} h^{-1}$ and the parameter estimates for enzyme reactivation (K_r) and aging (K_a) were held constant at the values determined for chlorpyrifos-oxon (Timchalk et al., 2002b), and are

presented in Table 3. The PBPK/PD model provided a reasonable simulation of plasma cholinesterase and BuChE inhibition; in both cases achieving maximal inhibition between 3–6 h post-dosing. With regards to RBC AChE inhibition, the PBPK/PD model reasonably simulated the inhibition time-course achieving maximal inhibition at ∼8 h post-dosing and little enzyme recovery though 24 h post-dosing.

Selected brain samples from the animals dosed with the target of 100 mg/kg and additional animals dosed with 15 and 500 mg/kg were analyzed for AChE activity and the experimental results and model simulations are presented in Fig. 6. The data demonstrated a clear dose-dependent inhibition of AChE with maximum inhibitions of 20, 70 and 90% of control activity for the 15, 100 and 500 mg/kg dose groups. The K_i used to describe the inhibition was assumed to be equal to the K_i determined for AChE in plasma, and the K_r and K_a were likewise held constant as previously described. Taken in its entirety, the model fits to this data are reasonable. The model underpredicts brain inhibition at earlier timepoints from the lowest dose (similar to blood and RBC esterase inhibition). At the 500 mg/kg dose, inhibition is essentially maximal, and the overprediction of inhibition relative to the 6 h data point reflects the difference between experimentally determinable percentage inhibition and maximal inhibition mathematically estimated by the model.

Oral dosing with DZN resulted in a dose-dependent reduction in both total cholinesterase and BuChE activity in the diaphragm (Fig. 7). BuChE activity dropped to ≤20% of control by 6–12 h and remained depressed over the 24 h period following the 100 mg/kg target dose. Total diaphragm cholinesterase was inhibited to a lesser extent than was BuChE alone, with maximal inhibition of approximately 40% of control by 6 h post-dosing. PBPK/PD model parameters for AChE and BuChE enzyme activity and inhibition were held constant based upon previous data fits (see Fig. 5) and were not optimized specifically for the diaphragm. Parameters optimized for brain and blood resulted in a reasonably good simulation of both the total cholinesterase and BuChE inhibition kinetics in this tissue.

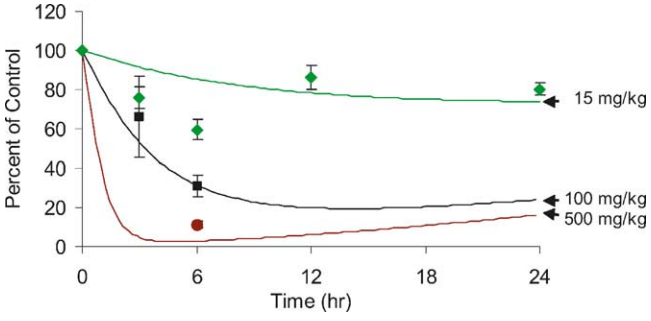

Fig. 6. Experimental data (symbols) and simulations (lines) for the inhibition of brain AChE in Sprague–Dawley rats administered DZN by oral gavage at doses of 15 (◆), 100 (■), and 500 (●) mg/kg. The data represent the mean ± S.D. of five animals per treatment group.

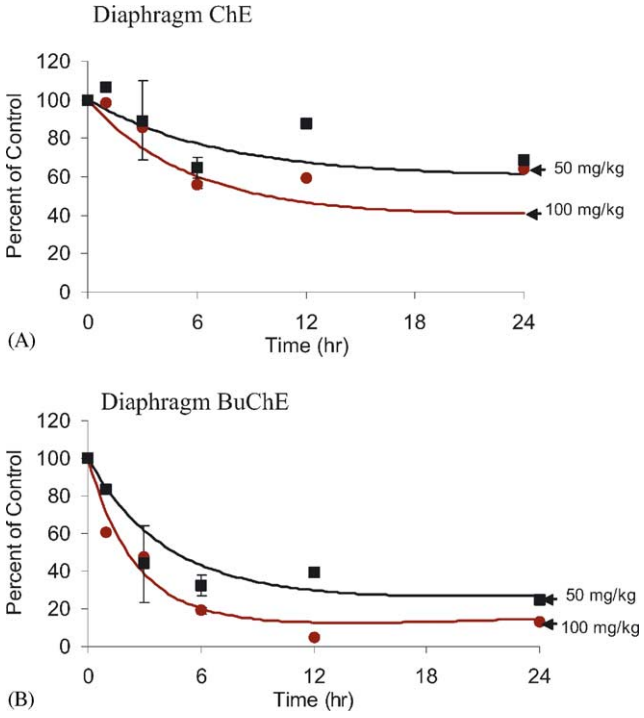

Fig. 7. Experimental data (symbols) and simulations (lines) for the inhibition of diaphragm total cholinesterase (ChE) and BuChE in Sprague–Dawley rats administered DZN by oral gavage at doses of 50 (■) and 100 (●) mg/kg. The data represent the mean ± S.D. of five animals per treatment group.

Model Validation from the Open Literature

To further evaluate the PBPK/PD model response, available dosimetry and dynamic data were obtained from the literature and the PBPK/PD model was appropriately modified to accommodate alternative routes of administration. Plasma DZN concentrations have been reported following i.v. and oral exposures (Wu et al., 1996) and i.p. exposures (Tomokuni et al., 1985). Wu et al. (1996) emulsified DZN in a 5% Tween 20:saline vehicle to administer 10 and 80 mg/kg doses for i.v. and oral studies, respectively. Oral absorption parameters were optimized for this vehicle (see Table 2). As was observed in the earlier model for chlorpyrifos, using a single first-order process to describe oral absorption resulted in a more rapid rise to peak concentrations than the data suggested. Therefore, oral

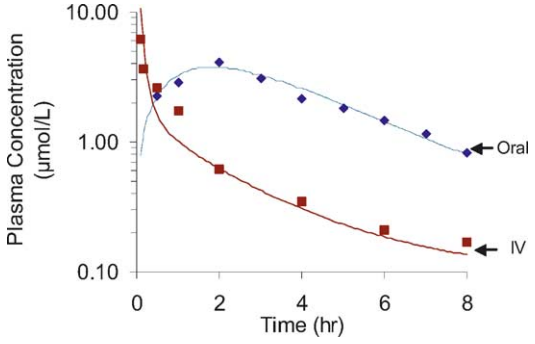

Fig. 8. Experimental data from Wu et al. (1996) and simulations (lines) for the concentration of DZN in the plasma of Sprague–Dawley rats administered DZN by oral gavage or i.v. administration at doses of 80 and 10 mg/kg, respectively. The fit of the model to estimate blood DZN and cholinesterase (see Fig. 10) was improved using a dose i.v. of 15 mg/kg.

absorption for this vehicle was described using a two-compartment gastrointestinal tract model as described previously (Staats et al., 1991; Timchalk et al., 2002b). The time-course of DZN in the blood following oral and i.v. administration and the model simulations are presented in Fig. 8. The time-course of the blood DZN for the 80 mg/kg dose is comparable to the results observed in the current study following doses of 50 and 100 mg/kg (see Fig. 3), which were accurately simulated by the PBPK/PD model. The peak blood concentration, however, was ~4× greater in this study. To fit the higher peak, the description of the transfer to the intestinal compartment and from that compartment into the blood were much faster (Table 2). The fraction of oral absorption was equivalent to the current study at 80%.

Following i.v. administration (Wu et al., 1996), a more biphasic kinetic profile was observed, with the terminal phase (3–8 h post-dosing) paralleling the response following oral administration (Fig. 8). To fit the data, a slightly higher dose than the reported target (10 mg/kg) was employed. The fit of the model to the data is shown with a 15 mg/kg estimated delivered dose. Dosing of an emulsified solution containing Tween may be difficult and may have result in higher dosing than anticipated.

An i.p. absorption rate constant (0.3 h^{-1}) was optimized to fit the data of Tomokuni et al. (1985) from a 100 mg DZN/kg dose, but only after the dose adjustment of 60 percent. The use of a percentage absorbed through the i.p. route is unusual; however, it was necessary to fit the data. The time-course of plasma, liver, and brain DZN concentration along with plasma cholinesterase inhibition were assessed and the data and model simulations are presented in Fig. 9. Peak

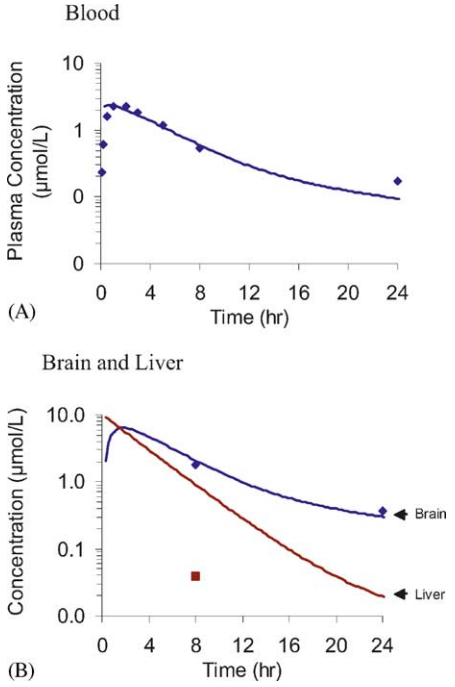

Fig. 9. Experimental data from Tomokuni et al. (1985) and simulations (lines) for the concentration of DZN in (A) plasma, and (B) brain (◆), and liver (■) of rats administered DZN by i.p. administration at a dose of 100 mg/kg.

plasma DZN concentrations were achieved rapidly (within 1 h post-dosing), and the plasma time-course was comparable to that observed following the 100 mg/kg oral administration in the current study (see Fig. 3). Again, the PBPK/PD model accurately simulated the DZN plasma time-course over 24 h post-dosing. At 8 and 24 h post-dosing DZN concentrations in brain were approximately 1.9 and 0.4 µmole/L, respectively, and the model did a good job of predicting these concentrations. The concentration of DZN in liver at 8 h, however, was considerably lower than predicted by the model.

Inhibition kinetics of cholinesterase were also described in these two studies (Tomokuni et al., 1985; Wu et al., 1996). The data of Wu et al. (1996) and Tomokuni et al. (1985) suggest a higher inhibition of RBC AChE than total plasma cholinesterase (Figs. 10 and 11). This is inconsistent with the model, which predicts more similar plasma cholinesterase inhibition relative to RBC inhibition. The data of Wu et al. (1996) was generated in male Wistar rats, compared to the Sprague–Dawley rats employed in these studies, and methods used to measure esterase activity were different.

At these concentrations, the model was more sensitive to estimations of K_m for the metabolism of DZN to the oxon than to K_i rates for inhibition of plasma

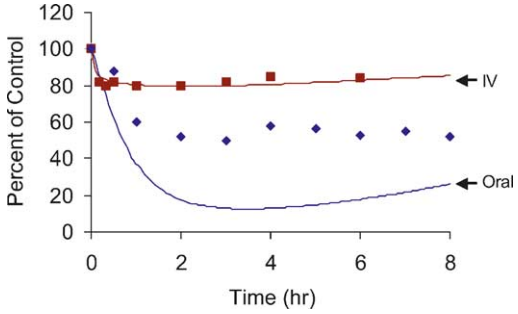

Fig. 10. Experimental data from Wu et al. (1996) and simulations (lines) for the inhibition of plasma total cholinesterase after oral and i.v. dosing with DZN to Wistar rats in a Tween 20:saline vehicle.

cholinesterase. The fit of the plasma inhibition data from Wu et al., was improved considerably by doubling the K_m as assessed using the Maximum Log Likelihood Function (LLF) of Simusolv™ (data not shown). The LLF of Simusolv gives a percent variation explained, which is frequently used as a criteria to assess the quality of the model fit to the data, with 100% indicating a perfect fit. The LLF parameter was improved from less than 80 to over 95% when the K_m for the metabolism of DZN to the oxon is doubled for these simulations.

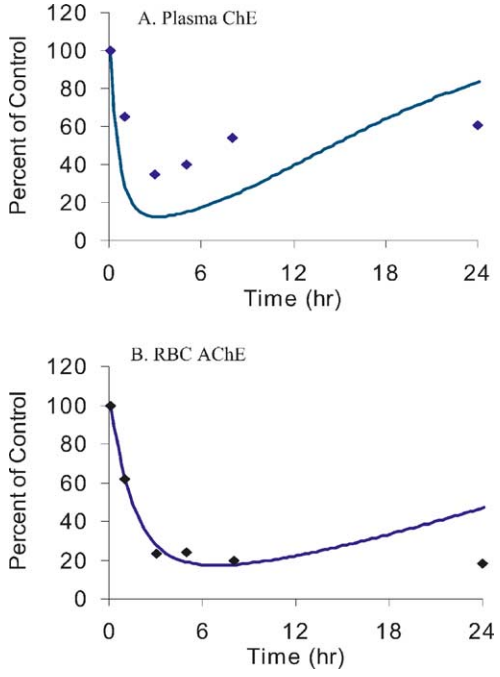

Fig. 11. Experimental data from Tomokuni et al. (1985) and simulations (lines) for the inhibition of (A) plasma total cholinesterase (ChE) and B) RBC AChE after i.p. dosing with 100 mg/kg DZN.

Model Fit against Human Oral and Dermal Data

To evaluate the capability of the PBPK/PD model to simulate the DZN dosimetry in humans, dosimetry data was sought. Only a recently reported controlled human DZN dermal and oral pharmacokinetic study was found, and results from this study were modeled (Garfitt et al., 2002). Human-specific physiological parameters were applied to the model (see Table 2).

Oral and dermal absorption parameters were optimized to fit the urinary elimination of combined diethylphosphate and diethylthiophosphate following a single oral exposure to 11 μg DZN/kg administered in 200 mL of water and an occluded dermal dose of 100 mg to five volunteers (four men and one woman). The kinetics of the combined diethylphosphate and diethylthiophosphate metabolites should be similar to those of IMHP (see Fig. 1), so a one-compartment model was added to the PBPK model, constructed on the same principles of the IMHP compartment, to describe the combined diethylphosphate and diethylthiophosphate kinetics. To fit the oral elimination data and decrease the number of variables necessary to optimize based on the limited data set, intestinal absorption parameters and fractional absorption were set to 0. Only oral absorption (K_{as}) and urinary elimination were fit to the data. All other parameters were held constant from the parameters optimized in the rat model. The optimized oral absorption rate was considerably higher than estimated in the rat, at 0.32 h^{-1}, and a very fast urinary elimination rate of 12 h^{-1} was needed (Fig. 12A). Using the assumption that the urinary elimination rate was reasonably accurate, an estimation of dermal absorption rate was achieved. The dermal dose was applied in 400 μl of ethanol over 80 cm^2 of skin (inner forearm) and was maintained on the skin for 8 h. An optimized skin permeability coefficient (K_P) of 1.3×10^{-4} cm/h resulted in a good fit to the data (Fig. 12B), this is similar to the K_P calculated for chlorpyrifos (Timchalk et al., 2002b; Table 4). Based on these assumptions, the fit of the PBPK/PD model to the oral and dermal absorption data was good, with more than 95% of the variability of the data explained by optimizing the K_P using the LLF function of Simusolv™, but this is to be expected since model parameters were optimized to these data sets.

DISCUSSION

The potential toxicity of an OP insecticide is dependent upon a combination of the amount delivered to the

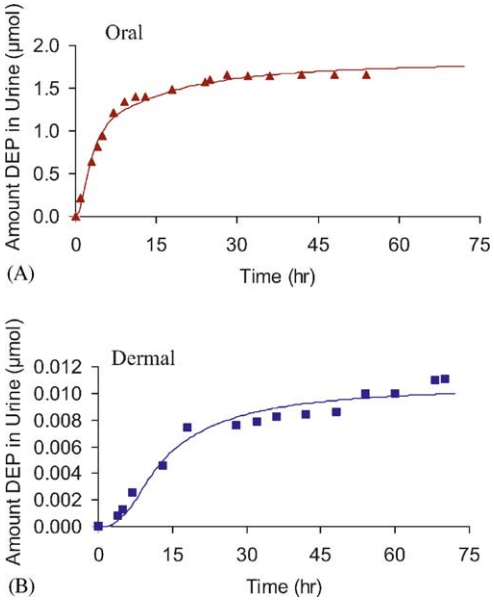

Fig. 12. Experimental data from Garfitt et al. (2002) and simulations (lines) for the urinary elimination of diethylphosphates following oral (11 µg/kg) and dermal (3.5 mg/kg) exposures in human volunteers.

target systems and the balance between bioactivation and detoxification (Timchalk, 2001). The neurotoxicity of DZN is primarily mediated through its toxic metabolite, DZN-oxon, and its ability to effectively inhibit AChE in nerve tissues. This PBPK/PD model was developed using the framework from a recently published PBPK/PD model for chlorpyrifos (Timchalk et al., 2002b) as a quantitative tool for assessing DZN dosimetry and cholinesterase inhibition in rats and humans. These PBPK/PD approaches are ideally suited for assessing dosimetry and biological responses following exposures and the development of ''family'' models that can be used for related chemicals or metabolites is an important expansion of this capability (Barton et al., 2000).

To provide needed data on DZN dosimetry and cholinesterase inhibition for model development, rat pharmacokinetic/pharmacodynamic studies were conducted. In addition, available published rat and human kinetic and dynamic studies were used to further validate the PBPK/PD model. Overall, this PBPK/PD model successfully predicts plasma DZN and IMHP and urinary IMHP kinetics, and cholinesterase inhibition kinetics in plasma, RBC, diaphragm and brain following DZN exposure from several routes. This model also was used to predict urinary elimination of combined diethylphosphate and diethylthiophosphate from dermal and oral exposures in human volunteers (Garfitt et al., 2002).

Table 4
Comparison of model parameterization for DZN and chlorpyrifos

Parameter	Diazinon	Chlorpyrifos[c]
Metabolic constants[a]		
CYP450 parent-to-oxon (liver)		
$K_{m,1}$ (µmole/L)	25	2.9
$V_{max,C1}$ (µmole/(h kg))	14	80
CYP450 DZN/CPF-to-IMHP/TCP[b]		
$K_{m,2}$ (µmole/L)	200	24
$V_{max,C2}$ (µmole/(h kg))	180	273
PON oxon-to-IMHP/TCP (liver)		
$K_{m,3}$ (µmole/L)	270	240
$V_{max,C3}$ (µmole/(h kg))	63000	74421
Oral absorption parameters		
K_{aS} (stomach; h^{-1})	0.068	0.01
K_{aI} (intestine; h^{-1})	0.058	0.50
K_{sI} (transfer stomach-intestine; h^{-1})	0.21	0.50
F_a (fractional Abs.; %)	0.80	0.80
Dermal absorption parameters		
K_p (permeability coefficient; cm/h)	1.3×10^{-4}	4.8×10^{-5}
Bimolecular inhibition rate (µmole/h)		
K_i all tissues AChE	525	243
K_i all tissues BuChE	1700	2000
K_i all tissue carboxylesterase	0.5	20

[a] Timchalk et al. (2002b).
[b] CPF—chlorpyrifos, TCP—trichloropyridinol, the inactive metabolite of chlorpyrifos.

Blood levels of DZN and IMHP were quantified from the animals in the 50 and 100 mg/kg dose levels and used to optimize oral absorption parameters. Blood levels were not quantified from the 15 mg/kg dose groups due to analytical limits of detection. The model was validated using blood concentration data from the published literature following i.v., i.p. and oral dosing. However, to fit the i.p. dosing data, a fractional uptake of 60% was added to the model. A fractional i.p. dose is not typically used as the dose is usually thought of as 100% absorbed. This fractional uptake was needed no only to fit the blood and brain dosimetry data, but also to fit the plasma cholinesterase inhibition data. The fit of the model to these multiple data sets requiring this unusual fractional absorption may suggest a depot or binding at the dosing site, and would potentially be an important opportunity for further studies. Interestingly, recent work by Domoradzki et al. (2004) has shown that the majority of a dose of chlorpyrifos injected subcutaneously in a DMSO vehicle remained at the injection site for an extended period of time. Overall, the PBPK/PD model reasonably simulated both the DZN dosimetry and cholinesterase inhibition time-course data from the current study and from previously published studies in which animals were exposed to single oral, i.v., and i.p. doses of DZN (Tomokuni et al., 1985).

Previous studies have indicated that DZN is extensively metabolized, with IMHP and hydroxylated metabolites of IMHP representing the major metabolites (Mücke et al., 1970; Iverson et al., 1975; Poet et al., 2003). The results of the current pharmacokinetic and pharmacodynamic study indicate that DZN is rapidly absorbed following oral administration and likewise undergoes extensive metabolism with IMHP accounting for ~30% of the dose recovered in the urine by 24 h post-dosing, which is consistent with ~23% of the dose being recovered as IMHP in the urine following oral administration of a 4 mg/kg DZN dose (Mücke et al., 1970). Peak levels of both DZN and IMHP in blood were achieved by 3 h post-dosing. In addition, over the dose-range evaluated, the kinetics of both DZN and IMHP were linear. To fit the urinary elimination of IMPH, a first-order non-specific loss of IMHP within the compartment was added to the model to account for potential further metabolism of IMHP. There is evidence that homologous metabolites of similar OP pesticides, such as chlorpyrifos, undergo glucuronidation in rats (Bakke et al., 1976) and humans (Nolan et al., 1984) and a glutathione metabolite of DZN has been identified in houseflys and pillwort plants (Clark et al., 2003; Ding and Yeo, 1986).

A number of in vivo studies in both animals and humans have suggested that the oral bioavailability of OP insecticides is significantly less than 100%. Braeckman et al. (1983) reported that only 1–29% of orally administered parathion was bioavailable in dogs. The oral bioavailability of chlorpyrifos from a corn oil vehicle was 80% in rats (Timchalk et al., 2002b). In humans, the bioavailability of orally administered chlorpyrifos ranged from as low as 20–35 to 70% depending upon the physical form of the CPF when administered (Nolan et al., 1984; Timchalk et al., 2002b). Wu et al. (1996) suggested that only 35% of the 80 mg/kg oral dose was systemically bioavailable; the PBPK model estimation indicated an 80% oral bioavailability fit both the data from the current study and the data from Wu et al. These results with DZN are consistent with the variability seen when evaluating the oral bioavailability of other related OPs such as chlorpyrifos and parathion (Timchalk et al., 2002b; Braeckman et al., 1983). It has recently been suggested that intestinal metabolism could result in significant first-pass detoxification effectively decreasing the oral bioavailability of these OPs (Poet et al., 2003). Cook and Shenoy (2003) used single-pass intestinal perfusion techniques and recently reported that chlorpyrifos was >99% absorbed in the intestines. This coupled to the recent finding of Poet et al. (2003) that demonstrated intestinal CYP450 and PON metabolism of chlorpyrifos suggests that localized intestinal metabolism may account for the lower systemic bioavailability of chlorpyrifos and related OPs like DZN. The question of bioavailability is of critical importance, particularly when interpreting cholinesterase response in the absence of understanding how much of the DZN was systemically available; hence DZN pharmacodynamic response data should include concurrent bioavailability assessment and further experimentation is needed.

The 15–500 mg/kg DZN doses from this focused in vivo pharmacokinetic study were generally well tolerated although the limited number of animals administered the 500 mg/kg dose did appear to display mild signs of excessive cholinergic stimulation (i.e. increased urination/defecation; lethargy; soiled fur). The lethal oral dose for DZN was reported to be 2000 mg/kg (Takahashi et al., 1991), 4-times greater than the maximal dose delivered in the current study. Even lacking overt toxicity, esterase inhibition was measured at even the lowest dose. Although no attempt was made to quantify the formation of DZN-oxon, there was an inhibition of cholinesterase activity in all tissues sampled over the dose range evaluated, which is

consistent with the model predicted levels of DZN-oxon formed. No in vivo or in vitro K_i values for DZN-oxon were available. Apparent K_i values for chlorpyrifos inhibition of AChE and BuChE have been reported (Timchalk et al., 2002b) and were used as starting parameters for optimizations. Apparent K_i for these enzymes should be consistent, regardless of tissue; therefore, optimizations in this model took advantage of investigating several tissues (plasma, RBC, brain, and diaphragm) to validate a single K_i value for cholinesterase inhibition in all tissues concurrently. The model accurately reflected the overall trends associated with plasma, RBC, brain, and diaphragm cholinesterase activities. Using the LLF function of Simusolv™, all fits were 80% or better to any given data set, with the exception of data from diaphragm cholinesterase inhibition. The least amount of background data was known for this tissue.

Relative sensitivities of the B-esterases to DZN exposure were BuChE > AChE > carboxylesterase, which follows the same trend observed previously for chlorpyrifos (Timchalk et al., 2002b). Relative to chlorpyrifos, DZN estimated apparent K_i were lower for BuChE and carboxylesterase, but 3-times higher for AChE (Table 4). The sensitivity of BuChE was higher than the sensitivity of AChE to inhibition following treatment with diisopropylfluorophosphate (Gearhart et al., 1990) and chlorpyrifos (Amitai et al., 1998; Timchalk et al., 2002b). Likewise, in the current study, BuChE was slightly more sensitive than AChE to the inhibitor effects of DZN-oxon since plasma and diaphragm cholinesterase (AChE + BuChE) inhibition were less than BuChE inhibition alone (Figs. 5 and 7). To reasonably simulate this response, the bimolecular inhibition rate constants (K_i) optimized to fit the data were 525 and 1700 $\mu M^{-1}\,h^{-1}$ for AChE and BuChE, respectively. The model predictions for apparent K_i were based solely on model-predicted levels of DZN-oxon, however, there are limited reports of potential other DZN metabolites with cholinesterase inhibitory potential (Imaizumi et al., 1993). Thus, the apparent K_i may be a composite of more than just inhibition by DZN-oxon.

While the physiological purpose of AChE in the nervous system has been well described (Wilson, 2001), the role of BuChE has not been fully determined, although several investigators suggest that BuChE inhibition is a significant non-enzymatic detoxification pathway that protects against AChE inhibition by OPs (Sultatos, 1994; Chambers et al., 1990; Yang and Dettbarn, 1998). Since BuChE is more sensitive to OP inhibition, Amitai et al. (1998) proposed that it could be given intravenously as an exogenous scavenger against AChE inhibition, and recent work in our laboratory has suggested that BuChE is a potential target enzyme for OP insecticide biomonitoring for nontraditional matrixes such as saliva as well as in plasma, where it is routinely evaluated (Kousba et al., 2003).

Although the model successfully estimated brain cholinesterase inhibition (Fig. 6), it under predicted brain DZN concentrations reported by Tomokuni et al. (1985); (Fig. 9). It is feasible that other processes that are more complicated than simple solubility, which is described using the partition coefficient, may be involved in determining the amount of DZN and DZN-oxon in the brain. For example, it has been previously reported using in vitro metabolism studies that the brain was capable of CYP450 metabolism of chlorpyrifos to chlorpyrifos-oxon, suggesting that localized metabolism could contribute to brain dosimetry for the oxon (Chambers and Chambers, 1989). Conversely, Van Tellingen (2001) suggested that the activity of p-glycoproteins within the blood:brain barrier may function to decrease the ability of many compounds, like DZN-oxon, to penetrate the brain based on their lipophilicity as determined by their octanol/water partition coefficient. In this regard, the related OP insecticide chlorpyrifos-oxon has been shown to be transported by brain p-glycoproteins (Lanning et al., 1996), making it plausible that DZN-oxon may likewise be transported by p-glycoprotein. Although the use of partition coefficients without modifications result in good estimation of cholinesterase inhibition, indicating that predicted DZN-oxon levels are reasonably estimated by the model, the inability of the model to predict the brain DZN concentrations reported by Tomokuni et al. (1985) suggest the need for further research.

In the process of refining the model to fit the available data, several key model parameters that impact the model fit to data sets were noted. The parameter with the strongest affect to data fit across the most scenarios was plasma protein binding of DZN and, to a slightly lesser extent, DZN-oxon. The extent of plasma protein binding reported by Wu et al. (1996) was employed in this model and not varied. An additional parameter that was found to only be important for some data sets was the Michaelis–Menten constant for the metabolism of DZN to DZN-oxon.

As previously noted, much of the model structure was based on the chlorpyrifos PBPK/PD model described by Timchalk et al. (2002b). Although the uses, metabolic scheme, and biological effects of these

two chemicals are analogous, DZN pharmacokinetics have some key differences. Most notably, the CYP450-mediated metabolism of DZN to either the active DZN-oxon or deactivated product, IMHP, have much lower affinities (higher K_M) than for either the activation or deactivation of chlorpyrifos (Table 4). In addition, the DZN bimolecular inhibitory rate constant for BuChE is lower than these constants are for chlorpyrifos. The net effect is a lesser extent of inhibition of cholinesterase following exposures to DZN compared to chlorpyrifos. In particular, decreasing the K_M for the metabolism to DZN-oxon would result in an increase in the amount of DZN-oxon and concomitantly a drastically higher inhibition of cholinesterase. The other kinetic differences between the two chemicals have less influence on model-prediction of esterase inhibition. This suggests that the toxicity of DZN will be much lower than that of chlorpyrifos, due mostly to the amount of bioactivation of the parent pesticide. The oral LD_{50} for chlorpyrifos in rats is 95–270 mg/kg whereas the LD_{50} for DZN has been reported to be between 76 and 415 mg/kg in rats depending on formulation, gender, and species (ATSDR, 1996). It has been suggested that the earlier formulations of DZN were more toxic due to breakdown products in the dosing solutions. LD_{50} estimations from more recent formulations (1980–1996) range from 300–460 mg/kg. In this study, all of the five animals dosed with 500 mg/kg survived and showed only minor overt toxicity.

Occupational and environmental exposures to OPs are likely primarily associated with the dermal route. However, evidence indicates that DZN is not well absorbed through the skin since less than 4% of the DZN dermally applied to human volunteers for 24 h was absorbed (Wester et al., 1993). Other OPs also show limited dermal absorption (Franklin, 1984; Griffin et al., 1999; Nolan et al., 1984; Timchalk et al., 2002b; USEPA, 1992; Wester et al., 1983). In the current PBPK/PD model, the absorption of DZN from dermal application in human volunteers was described using a permeability coefficient of 1.3×10^{-4} cm/h. The permeability coefficient used for DZN is similar to the value (4.8×10^{-5} cm/h) used to describe the absorption of chlorpyrifos (Timchalk et al., 2002a,b).

Garfitt et al. (2002) found no cholinesterase inhibition in the plasma of the human volunteers following oral and dermal exposures. Likewise, the PBPK/PD model predicts no inhibition (predicted activity is greater than 99% of control) following either the oral or dermal exposures in plasma, RBC, diaphragm, or brain (data not shown). Therefore, at these exposure levels (11 μg/kg oral and approximately 3.5 mg/kg dermal), cholinesterase inhibition in blood would not be a sufficient biomarker of exposure. The lack of cholinesterase inhibition also suggests that these exposure levels may not result in any adverse effects in humans. The effects of repeated exposures at these low levels is a potential area for further research.

In summary, this PBPK/PD model is capable of quantifying target tissue dosimetry and dynamic response in rats and humans and can be used to link metabolism to cholinesterase inhibition across species and strengthen the biological base for risk assessments. The capability of the model to accurately predict dosimetry and cholinesterase inhibition is limited by the accuracy of the model parameters and the limitations of the experimental data. Additional research is needed to better understand the potential role of gut metabolism and protein binding in modifying dosimetry particularly following low dose exposures. In addition, better characterization of the bimolecular inhibition rate constants and associated reactivation and aging rates for the interaction of DZN-oxon with B-est would be helpful for future model refinement. With the development of this PBPK/PD model for DZN a future aim will be to link this model with the chlorpyrifos model to assess the pharmacodynamic responses from exposures to a mixture of the two chemicals.

ACKNOWLEDGEMENTS

This publication was supported by grant 1 R01 OH03629-01A2 from Centers for Disease Control and prevention (CDC). Its contents are solely the responsibility of the authors and do not necessarily represent the official views of CDC.

REFERENCES

Aldridge WN. The nature of the reaction of organophosphorus compounds and carbamates with esterases. Bull World Health Organ 1971;44:25–30.

Amitai G, Moorad D, Adani R, Doctor BP. Inhibition of acetylcholinesterase and butyrylcholinesterase by chlorpyrifos-oxon. Biochem Pharmacol 1998;56:293–9.

Bakke JE, Feil VJ, Price CE. Rat urinary metabolites from O,O-diethyl-O-(3,5,6-trichloro-2-pyridyl) phosphorothioate. J Environ Sci Health B 1976;11:225–30.

Barton HA, Deisinger PJ, English JC, Gearhart JN, Faber WD, Tyler TR, Banton MI, Teeguarden J, Andersen ME. Family approach for estimating reference concentrations/doses for series of related organic chemicals. Toxicol Sci 2000;54:251–61.

Braeckman RA, Audenaert F, Willems JL, Belpaire FM, Bogaert MG. Toxicokinetics of methyl parathion and parathion in the dog after intravenous and oral administration. Arch Toxicol 1983;54:71–82.

Brown RP, Delp MD, Lindstedt SL, Rhomberg LR, Beliles RP. Physiologicaly parameter values for physiologically based pharmacokinetic models. Toxicol Indust Health 1997;13: 407–84.

Butte W, Heinzow B. Pollutants in house dust as indicators of indoor contamination. Rev Environ Contam Toxicol 2002;175: 1–46.

Carr RL, Chambers JE. Acute effects of the organophosphate paraoxon on schedule- controlled behavior and esterase-activity in rats - dose- response relationships. Pharmacol Biochem Behavior 1991;40:929–36.

Chambers JE, Chambers HW. Oxidative desulfuration of chlorpyrifos, chlorpyrifos-methyl, and leptophos by rat brain and liver. J Biochem Toxicol 1989;4:201–3.

Clark AG, Shamaan NA, Sinclair MD, Dauterman WC. Insecticide metabolism by multiple glutathione S-transferases in 2 strains of the housefly, Musca-Domestica. Pesticide Biochem Physiol 2003;25:169–75.

Domoradzki JY, Marty MS, Hansen SC, Timchalk C, Mattsson JL. Effect of different dosing paradigms on the body burden of chlorpyrifos in neonatal Sprague-dawley rats. Toxicologist 2004;78:104.

Ding JL, Yeo LC. Conjugation of diazinon with glutathione, and gamma-glutamyl-transferase actibivities in Pilularia-Americana. Compar Biochem Physiol C 1986;85:413–7.

Ellman GL, Courtney KD, Andres Jr, V, Feather-Stone RM. A new and rapid colorimetric determination of acetylcholinesterase activity. Biochem Pharmacol 1961;7:88–95.

Fabrizi L, Gemma S, Testai E, Vittozzi L. Identification of the cytochrome P450 isoenzymes involved in the metabolism of diazinon in the rat liver. J Biochem Mol Toxicol 1999;13: 53–61.

Franklin CA. Estimation of dermal exposure to pesticides and its use in risk assessment. Can J Physiol Pharmacol 1984;62: 1037–9.

Garfitt SJ, Jones K, Mason HJ, Cocker J. Exposure to the organophosphate diazinon: data from a human volunteer study with oral and dermal doses. Toxicol Lett 2002;134: 105–13.

Gearhart JM, Jepson GW, Clewell III, HJ, Andersen ME, Conolly RB. Physiologically based pharmacokinetic and pharmacodynamic model for the inhibition of acetylcholinesterase by diisopropylfluorophosphate. Toxicol Appl Pharmacol 1990;106: 295–310.

Griffin P, Mason H, Heywood K, Cocker J. Oral and dermal absorption of chlorpyrifos: a human volunteer study. Occ Environ Med 1999;56:10–3.

Hackathorn DR, Brinkman WJ, Hathaway TR, Talbott TD, Thompson LR. Validation of A Whole-Blood Method for Cholinesterase Monitoring. Am Indust Hygiene Assoc J 1983;44: 547–51.

Imaizumi H, Nagamatsu K, Hasegawa A, Ohno Y, Takanaka A. Metabolism and toxicity of acid phsphate-esters, metabolites of organophosphorous insecticides, in rat. Jpn J Cancer Res 1993;39:566–71.

Iverson F, Grant DL, Lacroix J. Diazinon metabolism in the dog. Bull Environ Contam Toxicol 1975;13:611–8.

Jepson GW, McDougal JN. Physiologically based modeling of nonsteady state dermal absorption of halogenated methanes from an aqueous solution. Toxicol Appl Pharmacol 1997; 144:315–24.

Kousba AA, Poet TS, Timchalk C. Characterization of the in vitro kinetic interaction of chlorpyrifos-oxon with rat salivary cholinesterase: a potential biomonitoring matrix. Toxicology 2003;188:219–32.

Lanning CL, Fine RL, Sachs CW, Rao US, Corcoran JJ, Abou-Donia MB. Chlorpyrifos oxon interacts with the mammalian multidrug resistance protein, P-glycoprotein. J Toxicol Environ Health 1996;47:395–407.

Lassiter TL, Barone Jr, S, Padilla S. Ontogenetic differences in the regional and cellular acetylcholinesterase and butyrylcholinesterase activity in the rat brain. Brain Res Dev Brain Res 1998;105:109–23.

Lewis RG, Fortune CR, Blanchard FT, Camann DE. Movement and deposition of two organophosphorus pesticides within a residence after interior and exterior applications. J Air Waste Manag Assoc 2001;51:339–51.

Lotti M. Clinical toxicology of anitcholinesterase agents in humans. In: Krieger R, editor. Handbook of pesticide toxicology, vol. 2, 2001. p. 1043–85.

Ma T, Chambers JE. Kinetic parameters of desulfuration and dearylation of parathion and chlorpyrifos by rat liver microsomes. Food Chem Toxicol 1994;32:763–7.

MacIntosh DL, Kabiru CW, Ryan PB. Longitudinal investigation of dietary exposure to selected pesticides. Environ Health Perspect 2001;109:145–50.

Maxwell D, Brecht K, Eberle M. Correlation of invitro acetylcholinesterase (AChE) inhibition with invivo toxicity of organophosphorus agents. Abstr Papers of the Am Chem Soc 1987;194:173.

Mortensen SR, Chanda SM, Hooper MJ, Padilla S. Maturational differences in chlorpyrifos-oxonase activity may contribute to age-related sensitivity to chlorpyrifos. J Biochem Toxicol 1996;11:279–87.

Mucke W, Alt KO, Esser HO. Degradation of 14 C-labeled Diazinon in the rat. J Agric Food Chem 1970;18:208–12.

Nolan RJ, Rick DL, Freshour NL, Saunders JH. Chlorpyrifos: pharmacokinetics in human volunteers. Toxicol Appl Pharmacol 1984;73:8–15.

Poet TS, Thrall KD, Corley RA, Hui X, Edwards JA, Weitz KK, Maibach HI, Wester RC. Utility of real time breath analysis and physiologically based pharmacokinetic modeling to determine the percutaneous absorption of methyl chloroform in rats and humans. Toxicol Sci 2000;54:42–51.

Poet TS, Wu H, Kousba AA, Timchalk C. In vitro rat hepatic and intestinal metabolism of the organophosphate pesticides chlorpyrifos and diazinon. Toxicol Sci 2003;72:193–200.

Poulin P, Krishnan K. A tissue composition-based algorithm for predicting tissue:air partition coefficients of organic chemicals. Toxicol Appl Pharmacol 1996;136:126–30.

Ramsey JC, Andersen ME. A physiologically based description of the inhalation pharmacokinetics of styrene in rats and humans. Toxicol Appl Pharmacol 1984;73:159–75.

Staats DA, Fisher JW, Conolly RB. Gastrointestinal absorption of xenobiotics in physiologically based pharmacokinetic models. A two-compartment description. Drug Metab Dispos 1991;19: 144–8.

Takahashi H, Kojima T, Ikeda T, Tsuda S, Shirasu Y. Differences in the mode of lethality produced through intravenous and oral

administration of organophosphorus insecticides in rats. Fundam Appl Toxicol 1991;16:459–68.

Taylor P, Radic Z, Hosea NA, Camp S, Marchot P, Berman HA. Structural bases for the specificity of cholinesterase catalysis and inhibition. Toxicol Lett 1995;82–83:453–8.

Timchalk C, Kousba A, Poet T. Monte Carlo analysis of the human chlorpyrifos-oxonase (PON1) polymorphism using a physiologically based pharmacokinetic and pharmacodynamic (PBPK/PD) model. Toxicol Lett 2002a;135:51.

Timchalk C, Nolan RJ, Mendrala AL, Dittenber DA, Brzak KA, Mattsson JL. A Physiologically based pharmacokinetic and pharmacodynamic (PBPK/PD) model for the organophosphate insecticide chlorpyrifos in rats and humans. Toxicol Sci 2002;66:34–53.

Tomokuni K, Hasegawa T, Hirai Y, Koga N. The tissue distribution of diazinon and the inhibition of blood cholinesterase activities in rats and mice receiving a single intraperitoneal dose of diazinon. Toxicology 1985;37:91–8.

USEPA. Dermal exposure assessment: Principles and applications. 1992; EPA/600/8-91/011B, United States Environmental.

Van Tellingen O. The importance of drug-transporting p-glycoproteins in toxicology. Toxicol Lett 2001;120:31–41.

Wester RC, Maibach HI, Bucks DAW, Guy RH. Malathion percutaneous-absorption after repeated administration to man. Toxicol Appl Pharmacol 1983;68:116–9.

Wester RC, Sedik L, Melendres J, Logan F, Maibach HI, Russell I. Percutaneous absorption of diazinon in humans. Food Chem Toxicol 1993;31:569–72.

Wilson BW. Cholinesterases. In: Krieger R, editor. Handbook of pesticide toxicology, vol 2. Academic Press; 2001. p. 967–86.

Wu HX, Evreux-Gros C, Descotes J. Diazinon toxicokinetics, tissue distribution and anticholinesterase activity in the rat. Biomed Environ Sci 1996;9:359–69.

Yang RS, Hodgson E, Dauterman WC. Metabolism in vitro of diazinon and diazoxon in rat liver. J Agric Food Chem 1971;19:10–3.